Simultaneous Registration and Stiffness mapping of a Flexible Environment using Stiffness and Geometric Prior

R. A. Srivatsan[1], L. Wang[2], E. Ayvali[1], N. Simaan[2], H. Choset[1]

[1]*Robotics Institute, Carnegie Mellon University,*

[2]*Mechanical Engineering, Vanderbilt University*

rarunsrivatsan@cmu.edu

INTRODUCTION

In minimally invasive surgeries (MIS), surgeons have limited situational awareness of the surgical environment, making navigation a challenging task. Registration of preoperative images to intra-operative anatomy can help improve the situational awareness of the surgeon and validate if the surgery is going as per the preoperative plan. In this work, we use prior information about stiffness and geometry of the organ to develop an implementation for simultaneous registration and stiffness mapping.

While several imaging-based techniques [1], [2] and palpation-based techniques [3] have been used for registration, these methods tend to perform poorly when the organ geometry is rotationally symmetric, as in the case of liver, heart, etc. A rotationally symmetric object has multiple solutions for rotation and/or translation, resulting in an ambiguity in registration [4]. In other applications, this ambiguity is usually resolved by introducing an additional dimension such as surface texture [5], surface reflectance [6], etc.

In order to develop a formulation for registration that works reliably for any organ geometry, we extend the formulation of [3] by using a stiffness prior in addition to the geometric prior for resolving the ambiguity in registration. A prior stiffness map can be generated using elastography, physics based simulations or other complementary methods. Through experiments on a flat silicone organ with embedded stiff inclusions, we show that our method accurately estimates the registration as well as the stiffness map and outperforms the state of the art.

MATERIALS AND METHODS

To evaluate our algorithm we have used a custom designed Cartesian robot with an open architecture controller (see Fig. 1(a)). The robot end-effector is equipped with an ATI Nano43 F/T sensor. The end-effector is controlled using a hybrid motion/force controller implemented as in [7].

For the experiment, we used a silicone phantom organ with embedded stiff inclusions as shown in Fig. 1(b). A region of interest was chosen on the surface of the organ and several points in that region were probed. The phantom organ was lubricated to reduce the effect of friction during probing.

The robot was commanded to probe the organ up to a set depth along the normal direction and the applied force was recorded.

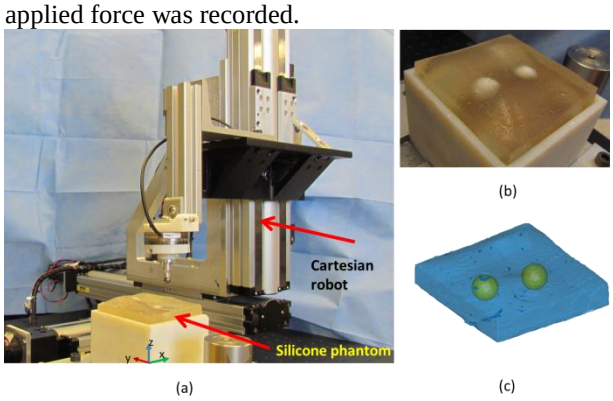

Fig. 1. (a) Cartesian robot setup for experiments. (b) Top view of the silicone phantom organ with embedded stiff inclusions. (c) CAD model of the organ and the stiff inclusions.

The force and position measurements, along with the CAD model of the organ and the prior stiffness map, were used to estimate the registation and the stiffness map of the organ.

Steps involved

Our formulation takes the following steps:

0. *Prior information gathering*: In this work the geometric prior is obtained by generating the CAD model of the organ and the inclusions from CT scans (see Fig. 1(c)). We generate the prior stiffness using a physics based simulation that assumes a linear stiffness model. The stiffness values are normalized and classified into two discrete levels, high and low stiffness, using Otsu method [8].
1. *Collection*: In the collection step, we collect sets of position-force measurements which correspond to probing of the same undeformed point on the surface of the organ. For example, $\left(\boldsymbol{p}_j^R, f_j\right)_i$ is a set of m measurements collected for the i^{th} probed point where $j = 1, \dots, m$ and $i = 1, \dots, n$. $\boldsymbol{p}_j^R, f_j$ are the position and force-magnitude measurements.
2. *Stiffness estimation*: We estimate the local stiffness by assuming a linear stiffness model and computing the slope of the best line that describes the variation of depth with the applied force.
3. *Correspondence*: The correspondence step involves finding points on the CAD model that map to the location of each of the undeformed points as

estimated from the sensor measurements. In order to ensure that a point corresponding to a high stiffness region on the model-frame is mapped to a point with high stiffness in the robot's frame, we normalize and classify the estimated stiffness map using [8] (Fig. 2(c) was generated from Fig. 2(a)). We choose the point on the CAD model that is closest and also has the same discrete stiffness level in the prior stiffness map.

4. *Minimization*: The optimal registration $\boldsymbol{T} \in SE(3)$ can be obtained from the following:

$$\boldsymbol{T} = argmin_{\boldsymbol{T}} \sum_{i=1}^{n} \left\| \boldsymbol{p}_i^C - \frac{\boldsymbol{n}_i^C(f_j)_i}{c_i} - \boldsymbol{T}\left(\boldsymbol{p}_j^R\right)_i \right\|^2 , (1)$$

Where $\boldsymbol{n}_i^C$ and $\boldsymbol{p}_i^C$ are the normal vector and the position of the probed point in the model's reference frame and c_i is the estimated stiffness. In this work, Eq. 1 is minimized using a least squares solver [4].

5. We loop between Step 3 and Step 4 until convergence or up to a fixed number of iterations.

RESULTS

The stiffness map estimated by our approach is shown in Fig. 2(a). Note that the two stiff inclusions are clearly visible in the stiffness map. In Fig. 2(d), black-diamond markers show the 180 points that were probed in the region of interest. Green-square markers show the initial guess for the location of the probed points. In Fig. 2(e), blue-star markers show the position as estimated by CMU [3]. Red-circular markers show the position estimated by our approach.

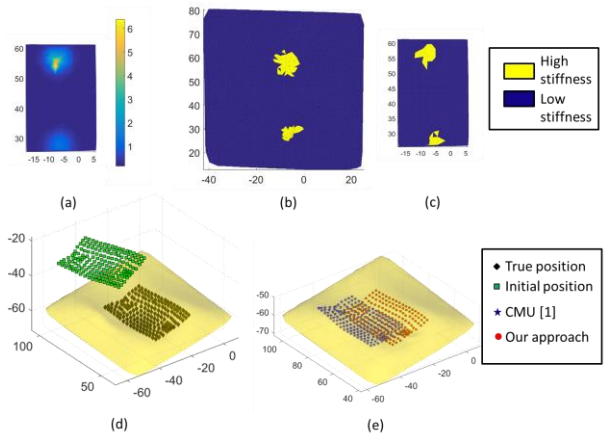

Fig. 2. (a) Estimated stiffness map (stiffness in N/mm). (b) and (c) Prior stiffness map and estimated stiffness map respectively, normalized and stiffness values classified to high and low stiffnesss levels. (d) Initial and true location of probed points. (e) Estimated location probed points.

Table 1: Comparison of registration results

	x (mm)	y (mm)	z (mm)	θ_x (deg)	θ_y (deg)	θ_z (deg)	RMS (mm)
Initial	0	0	0	0	0	0	-
Actual	-20	15	-10	11.46	-8.59	5.73	-
Our approach	-21	16.73	-9.1	11.28	-8.6	5.23	2.19
CMU [3]	-16.4	19.9	-14.8	15.45	5.84	8.16	7.74
ICP[1]	-18.9	20.5	-15.4	16.21	7.35	6.5	7.77

The estimated registration parameters are compared with ICP [1] and CMU [3]. Table 1 shows the RMS error for each of these methods for a representative example. Our approach estimates the registration parameters very accurately and the RMS error is within clinical requirements [9].

DISCUSSION

In this work, we developed a new implementation for simultaneous registration and stiffness mapping of an organ. In contrast to prior work, we have demonstrated successful registration in cases where the organ geometry is rotationally symmetric.

We use a stiffness prior in addition to a geometric prior for finding correspondences with the model frame and hence resolve the ambiguity in registration. By performing experiments on a silicone phantom organ we have shown that our approach can successfully register while estimating the stiffness map and outperform state of the art methods.

While we have used a simple experimental setup and phantom organ, as part of future work we plan to demonstrate the method on the da Vinci surgical robot probing *ex vivo* organs.

ACKNOWLEDGEMENT

This work has been funded through the National Robotics Initiative grants IIS-1426655 and IIS-1327566

REFERENCES

[1] P. J. Besl and N. D. McKay, "A method for registration of 3-D shapes," IEEE Transactions on Pattern Analysis and Machine Intelligence, vol. 14, pp. 239–256, 1992.

[2] M. V. Wyawahare, P. M. Patil, H. K. Abhyankar, et al., "Image registration techniques: an overview," IJSIP, vol. 2, no. 3, pp. 11–28, 2009.

[3] R. A. Srivatsan, E. Ayvali, L.Wang, R. Roy, N. Simaan, and H. Choset, "Complementary Model Update: A Method for Simultaneous Registration and Stiffness Mapping in Flexible Environments," In Proceedings of ICRA 2016.

[4] K. Arun, T. Huang, and S. Bolstein, "Least-Squares fitting of Two 3-D Point Sets," IEEE Transactions on Pattern Analysis and Machine Intelligence, vol. 9, no. 5, pp. 698–700, 1987.

[5] A. E. Johnson and S. B. Kang, "Registration and integration of textured 3D data," Image and vision computing, 17(2), pp. 135-147, 1999.

[6] L. Cerman, A. Sugimoto, and I. Shimizu. "3D shape registration with estimating illumination and photometric properties of a convex object," In Proceedings of Computer Vision Winter Workshop, 76–81, 2007.

[7] O. Khatib, "A unified approach for motion and force control of robot manipulators: The operational space formulation," IEEE Journal of Robotics and Automation, vol. 3, no. 1, pp. 43–53, 1987.

[8] N. Otsu. "A Threshold Selection Method from Gray-Level Histograms." Automatica 11 (1975): 285-296.

[9] C. A. Linte, J. Moore, and T. M. Peters, "How accurate is accurate enough? A brief overview on accuracy considerations in image-guided cardiac interventions," in Annual International Conference of the Engineering in Medicine and Biology Society, pp. 2313–2316, 2010.